Received 6 September 2019; | Revised XX September 2019; | Accepted XX September 2019

DOI: xxx/xxxx

ARTICLE TYPE

Lessons learned from 19 years of high-resolution X-ray spectroscopy of galaxy clusters with RGS†

Ciro Pinto*[1,2] | Andrew C. Fabian[3] | Jeremy S. Sanders[4] | Jelle de Plaa[5]

[1]ESTEC, ESA, Keplerlaan 1, 2201AZ Noordwijk, Netherlands
[2]IASF Palermo, INAF, Via U. La Malfa 153, I-90146 Palermo, Italy
[3]Institute of Astronomy, Cambridge, CB3 0HA, United Kingdom
[4]Max-Planck-Institut fur extraterrestrische Physik, Giessenbachstrasse 1, D-85748 Garching, Germany
[5]Netherlands Institute for Space Research, Sorbonnelaan 2, 3584 CA Utrecht, Netherlands

Correspondence
*Ciro Pinto, IASF Palermo, INAF, Via U. La Malfa 153, I-90146 Palermo, Italy. Email: ciro.pinto@inaf.it

The intracluster medium (ICM) contains the vast majority of the baryonic matter in galaxy clusters and is heated to X-ray radiating temperatures. X-ray spectroscopy is therefore a key to understand both the morphology and the dynamics of galaxy clusters. Here we recall crucial evolutionary problems of galaxy clusters unveiled by 19 years of high-resolution X-ray spectroscopy with the Reflection Grating Spectrometer (RGS) on board XMM-*Newton*. Its exquisite combination of effective area, spectral resolution and excellent performance over two decades enabled transformational science and important discoveries such as the lack of strong cooling flows, the constraints on ICM turbulence and cooling-heating balance. The ability of RGS to resolve individual ICM spectral lines reveals in great detail the chemical enrichment in clusters by supernovae and AGB stars. RGS spectra clearly showed that the ICM plasma is overall in thermal equilibrium which is unexpected given the wealth of energetic phenomena such as jets from supermassive black holes and mergers.

KEYWORDS:
X-rays: galaxies: clusters, galaxies: clusters: general, cooling flows, evolution, intergalactic medium.

1 | INTRODUCTION

The intracluster medium (ICM) embedded in the deep gravitational potentials of galaxy clusters is a unique laboratory where highly energetic astrophysical phenomena occur. Its thermodynamic and chemical properties witness the evolution of the individual galaxies as altered by several phenomena such as galaxy mergers, gas sloshing and feedback from active galactic nuclei (AGN). About a third of galaxy clusters shows a highly peaked density profile, which corresponds to the region where the central cooling time is significantly shorter than the age of the Universe and that of the clusters (cool core clusters, e.g. Hudson et al. 2010). In the absence of heating, this would imply the cooling of hundreds of solar masses of gas per year below 10^6 K (Fabian, 1994) for the massive clusters, with a consequent star formation rate of a similar order of magnitude. Spectral models of massive cooling flows of $100 \mathrm{s}\, \mathrm{M}_\odot\, \mathrm{yr}^{-1}$ were consistent with the shapes of spectra from low-resolution X-ray spectrometers on board early observatories like *ROSAT*, although some clusters showed breaks in the mass deposition rates (see e.g. Peres et al. 1998 and references therein). Absorption from cool gas within the cluster was invoked to explain some of the missing emission at the soft X-ray energies.

Star formation triggered by gas cooling is expected to enhance the metallicity of the intracluster medium and to complicate its chemical structure. Core-collapse supernovae are known to contribute to lighter elements such as O, Ne and Mg, while type Ia supernovae dominate the fraction of S, Fe, Ni and other heavy elements (see e.g. de Plaa et al. 2007). Nitrogen is most likely produced by AGB stars. The relative ratios of N, O and Ne to Fe (among the most abundant metals) are therefore the means to determine the star formation history of clusters.

Nowadays, the most commonly used X-ray spectrometers are charge-coupled device (CCD) cameras like those on board XMM-*Newton*, *Chandra* and *Suzaku* owing to their high effective area although low-to-medium spectral resolution (R =

†RGS is the Reflection Grating Spectrometer on board XMM-*Newton*.

$E/\Delta E \sim 10-50$). These detectors are very useful due to their 2D imagining capabilities and high-count-rate spectra, which enabled important discoveries such as the bubbles inflated by AGN jets (witnessing the effects of the supermassive black hole of the central brightest cluster galaxy, BCG, onto the surrounding ICM, e.g. Churazov, Forman, Jones, & Böhringer 2000 and Fabian, Sanders, Taylor, & Allen 2005) and the flat radial profiles of the abundances (suggesting an early enrichment or a complex mixing / cycle of the metals within the cluster, see e.g. Matsushita et al. 2007 and Urban et al. 2017).

However, CCD detectors are not able to detect and resolve individual X-ray emission lines, particularly those produced by high-ionisation ions of nitrogen (mainly N VII), oxygen (O VII-VIII), neon (Ne IX-X) and the Fe L complex (Fe XXIV or lower ionisation states), which are the main tracers of cooling flows. This causes large uncertainties in the estimates of temperatures and emissivities of cool gas phases and amount of cool gas.

High energy-resolution dispersive spectrometers (gratings) and micro-calorimeters were designed to constrain cooling flows and search for high levels of turbulent and bulk motions in the intracluster gas, which were expected given the wealth of highly energetic phenomena occurring in the cores and in the outskirts of clusters. Galactic mergers, gas sloshing and AGN jets are thought to generate motions for up to $\sim 500-1000$ km s^{-1} (see e.g. Ascasibar & Markevitch 2006; Lau, Kravtsov, & Nagai 2009 and Brüggen, Hoeft, & Ruszkowski 2005). This might release enough heat to balance cooling. The level of turbulence is crucial to identify any bias in mass measurements of clusters due to the assumption of hydrostatic equilibrium.

2 | XMM-*NEWTON* / RGS

Detailed astrophysics of X-ray sources often requires significantly higher spectral resolution ($R = E/\Delta E \sim 100-1000$). This has been offered, excluding the brief life of *Hitomi* (operating for five weeks and carrying a microcalorimeter, Hitomi Collaboration 2016) only by the grating spectrometers on board XMM-*Newton* (the Reflection Grating Spectrometer, RGS, see den Herder et al. 2001) and *Chandra* (the low / high transmission grating spectrometers, LETGS and HETGS).

Gratings have less applicability than CCDs due to limited imaging (mostly 1D) and count-rate (lower effective area) capabilities. They are therefore optimal for bright sources (Flux$_{0.3-2\,\mathrm{keV}} \gtrsim 10^{-12}$ erg s^{-1} cm^{-2}) and, particularly, those with small angular size ($\lesssim 1'$) since the gratings do not have a slit. For instance, the RGS spectral lines are broadened according to the law $\Delta\lambda = 0.138\,\Delta\theta$ Å$/m$, where $\Delta\lambda$ is the wavelength broadening, $\Delta\theta$ is the source extent in arc minutes and m is the spectral order. RGS is currently the ideal grating spectrometer for extended sources owing to its high spectral resolution ($R = E/\Delta E \sim 100-800$) and sufficient effective area ($\sim 20-100$ cm^2) in the soft X-ray energy range ($\sim 0.33-1.77$ keV) where a forest of spectral lines are produced by the K shells of some among the most abundant elements in the Universe such as C, N, O, Ne and Mg and the complex L shells of Fe and Ni.

3 | RGS UNIQUE CONTRIBUTIONS

We first focus on the major results in the astrophysics of galaxy clusters primarily driven by the capabilities of the RGS before moving to the synergies with other facilities.

3.1 | Cooling rates

The first light of RGS onto clusters of galaxies brought up a huge surprise. The observed cooling rates of cool-core clusters were much lower than the theoretical predictions and the previous measurements of CCD detectors, showing only modest levels of a few dozens M$_\odot$ yr^{-1} (see, e.g., Kaastra et al. 2001; Peterson et al. 2001; Tamura et al. 2001). Fig. 1 shows a comparison between the RGS spectra of some clusters with empirical (quasi-isothermal) models of gas in collisional equilibrium and cooling-flow models. The cooling-flow model is not a best fit, but calculated by merely taking the soft X-ray flux in the empirical model and using the standard isobaric temperature distribution. The cooling-flow models overpredict the strength of the Fe XVII-XVIII emission lines from the plasma at low temperatures. There is a remarkable lack of gas below $\sim 1-2$ keV (see also Sanders et al. 2008 and Liu, Pinto, Fabian, Russell, & Sanders 2019). Cooling rates are even lower below 0.5 keV as shown by the faint O VII lines recently discovered in elliptical galaxies and clusters (Pinto et al. 2016, 2014). In Sect. 4.3 we also show the comparison between the cooling rates measured in clusters through the RGS with indicators of star formation rates determined with facilities at low energies.

The X-ray emission lines in RGS spectra showed that the ICM plasma is overall in thermal equilibrium which was not obvious given the presence of energetic phenomena such as jets from supermassive black holes, mergers and cooling flows.

3.2 | Kinematics

Only since 2010s RGS has been used to place constraints on turbulence by measuring the velocity dispersion of the ICM, mainly due to the line broadening caused by the spatial extent of clusters. However, the line spatial broadening of clusters with X-ray core $\lesssim 1'$ is limited to a few hundred km s^{-1} and can be corrected through CCD surface brightness profiles.

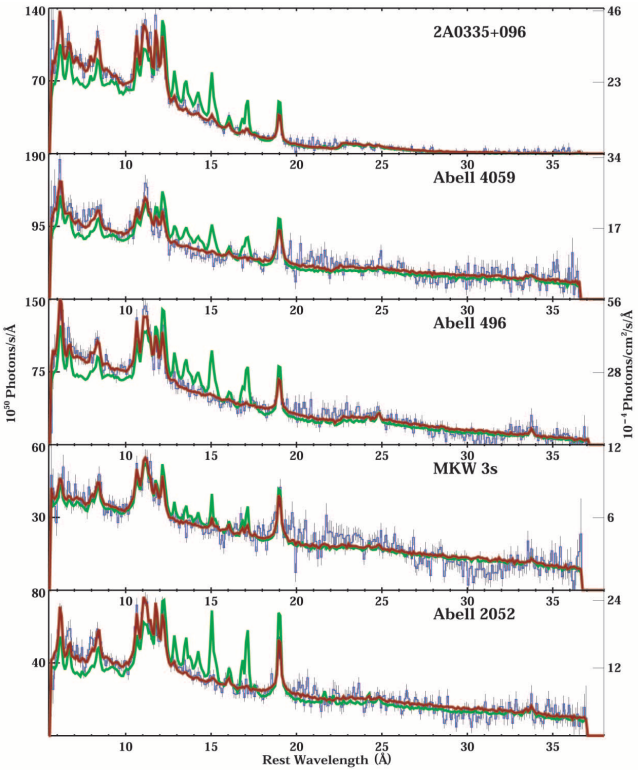

FIGURE 1 First RGS observations of galaxy clusters (Peterson et al., 2003). Comparison of the data (blue), the empirical best fit model (red), and the standard cooling-flow model (green). The latter overestimates emission lines from cool gas.

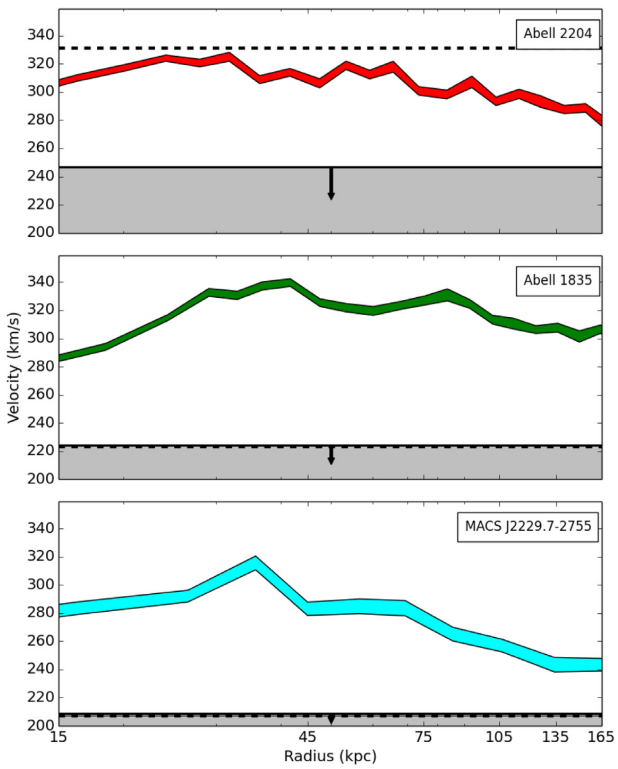

FIGURE 2 Constraints on turbulent velocities for three clusters of galaxies (Bambic et al., 2018). The coloured regions show the propagation velocity required to balance radiative cooling (1σ error). The dashed (solid) line shows the 90% upper limit on 1D turbulent velocities without (with) spatial broadening subtracted. This indicates that AGN turbulence alone is unable to balance radiative cooling in the inner core.

Sanders, Fabian, Smith, & Peterson (2010) placed the first 90% upper limit (274 km s^{-1}) on the velocity broadening of the luminous cool-core cluster A 1835 at redshift 0.25 with RGS spectra. Bulbul et al. (2012) constrained the turbulent motions in the compact core of A 3112 to be lower than 206 km s^{-1}. Sanders, Fabian, & Smith (2011) found turbulent broadening below 700 km s^{-1} for 30 clusters, groups, and elliptical galaxies observed with XMM-*Newton*/RGS, subsequently confirmed by Pinto et al. (2015) on nearby ($z \lesssim 0.08$) clusters using the CHEERS sample of 44 sources. They also showed that the upper limits on the Mach numbers are larger than the values required to balance cooling, suggesting that dissipation of turbulence may be high enough to heat the gas and prevent gas cooling (if turbulence is locally replenished).

Similar levels of turbulence have been constrained in giant elliptical galaxies with resonant scattering (see, e.g., Werner et al. 2009, de Plaa, Zhuravleva, Werner, Kaastra, & Churazov 2012, Pinto et al. 2016, Ogorzalek et al. 2017). When turbulence is low, the Fe XVII resonant line ($\lambda = 15$ Å) is optically thick and suppressed along the line of sight, while the 17 Å forbidden line remains optically thin. The comparison of their observed line ratio with simulations for different Mach numbers constrains the level of turbulence. This method is very efficient for cool ($kT < 0.9$ keV) giant elliptical galaxies rich in Fe XVII emission lines, but it is affected by the systematic uncertainty (up to ∼20%) in the line ratio. Currently, we cannot use this technique for clusters because they typically have higher ionisation lines (e.g. Fe XXV), which fall out of the RGS energy band. In a few years, studies of resonant scattering in clusters will be possible with *XRISM* (Guainazzi & Tashiro 2018) as its precursor, *Hitomi*, did for the sole observation of the Perseus cluster (Hitomi Collaboration, 2017).

Importantly, line broadening is less than $200 - 300$ km s^{-1} when the spurious spatial broadening is removed through the conversion of CCD surface brightness profiles into line spatial broadening (Pinto et al., 2015; Sanders & Fabian, 2013). This indicates that turbulence contributes to the total energy for less than ~ 5 % and is consistent with the measurements of *Hitomi* for Perseus (Hitomi Collaboration, 2016). Bambic et al. (2018) and Pinto et al. (2018) expanded this argument and showed that the propagation velocity is too low to achieve balance between gas cooling and heating via dissipation of turbulence (see Fig. 2), previously invoked by Zhuravleva et al. 2014 using surface brightness fluctuations. An additional source of heating may be sound waves (e.g. Fabian et al. 2017).

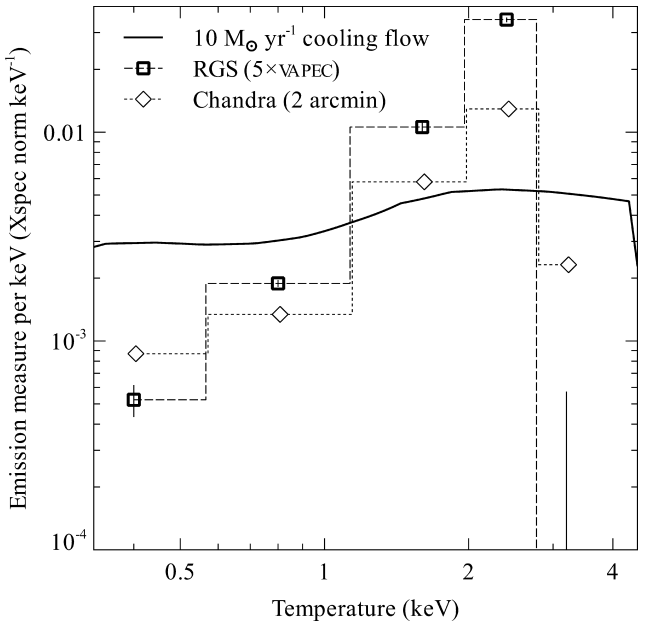

FIGURE 3 Comparison of the emission measures from RGS and Chandra observations of the Centaurus cluster core (Sanders et al., 2008). The solid line shows the expected distribution for a $10\,M_\odot\,yr^{-1}$ isobaric cooling flow.

3.3 | Multiphaseness

There was evidence for a multiphase ICM in early X-ray CCD spectra of galaxy clusters. Spatially-resolved spectroscopy indicates a complex morphology and multi-temperature gas (de Plaa et al., 2004; Frank, Peterson, Andersson, Fabian, & Sanders, 2013; Kaastra et al., 2004; Tamura et al., 2001). This is partly due to projection effects, because of the temperature gradient in the core. Deep RGS spectra of cool-core clusters provide the means from breaking some degeneracy through the detection of individual lines that enable to distinguish between different physical models. The results indicate that a powerlaw temperature distribution for the emission measure is favoured over a gaussian distribution (see Fig. 3 and Liu et al. 2019; Sanders et al. 2008; Werner, de Plaa, et al. 2006). This is confirmed by the fact that RGS spectra can be better modelled with 2 emission components in collisional ionisation equilibrium rather than with a gaussian temperature distribution (two APEC models in XSPEC [1] or two CIE models in SPEX [2], e.g., Pinto et al. 2015 and de Plaa et al. 2017) with the cooler component having a much lower emission measure.

3.4 | Chemical enrichment

As mentioned in Sect. 1, to unveil the history of chemical enrichment in clusters it is necessary to detect and resolve individual lines from ionic species of abundant elements. The RGS observations showed that AGB stars dominate the enrichment of nitrogen due to its high abundance measured with the bright N VII line in the RGS spectra of several clusters and giant elliptical galaxies (see e.g. Tamura et al. 2003, Buote, Lewis, Brighenti, & Mathews 2003, Sanders et al. 2008, Werner, de Plaa, et al. 2006). Werner, Böhringer, et al. (2006) and Grange et al. (2011) also measured the carbon abundance, confirming that the creation of nitrogen and carbon takes place in low- and intermediate-mass stars (see also de Plaa et al. 2007).

The detections of individual O VIII and Ne IX-X emission lines enabled accurate measurements of α/Fe abundance ratios in galaxy clusters. In most cases, the O/Fe and Ne/Fe abundance ratios - as measured with previous atomic databases - seemed to be sub-Solar [3] (e.g. Bulbul et al. 2012; Buote et al. 2003; de Plaa et al. 2004; Grange et al. 2011; Mernier et al. 2016b; Simionescu et al. 2009; Tamura et al. 2003; Werner, de Plaa, et al. 2006). On average, the relative fractions of type Ia supernovae are SN Ia / (SN Ia + SN cc) $\sim 25-45$ %, possibly larger than the Solar environment ($\sim 15-25$ %) and, therefore, suggest additional production of heavy elements from recent SN type Ia in the BCG. However, the uniformity of the O/Fe and Ne/Fe abundance ratios over more than an order of magnitude in mass range (from giant ellipticals to groups and then clusters of galaxies) and the lack of spatial gradients and distribution with the redshift indicate that either most metals were formed around $z \sim 2$ or that several phenomena such as sloshing and metal uplift by AGN bubbles redistributed the metals (see e.g. Mernier et al. 2016a, de Plaa et al. 2017).

4 | RGS SYNERGIES

4.1 | Synergies with X-ray CCD detectors

XMM-*Newton* observations of clusters have showed an excellent synergy between the capabilities of RGS in measuring the relative abundances of light α elements (C, N, O, Ne and Mg) with respect to iron and EPIC (both pn and MOS) in determining the absolute abundances (relative to hydrogen) of heavier elements (Si, S, Ar, Ca, Cr, Mn, Fe and Ni) owing to its higher sensitivity to the bremsstrahlung continuum (see Sect. 3.4).

4.2 | Synergies with X-ray calorimeters

RGS is even more efficient if used together with other high resolution spectrometers that cover the high-energy (2–10 keV)

[1] https://heasarc.gsfc.nasa.gov/xanadu/xspec/
[2] https://www.sron.nl/astrophysics-spex

[3] 'Solar' refers to the proto-Solar abundances of Lodders & Palme (2009).

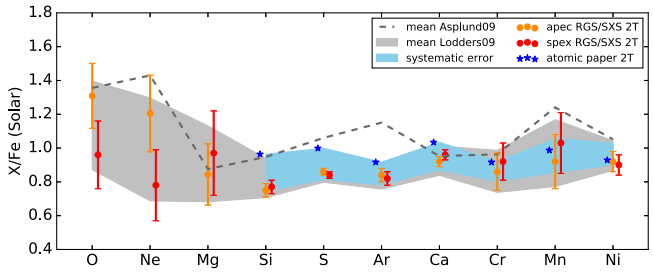

FIGURE 4 Abundance ratios measured for the Perseus cluster with XMM-*Newton*/RGS (O, Ne, Mg to Fe) and *Hitomi*/SXS (Si through Ni to Fe, Simionescu et al. 2019). The light blue strip is the systematic uncertainty on the *Hitomi* data. The grey strip includes both systematic and statistical uncertainties. The measured values are given with respect to the units of Lodders & Palme (2009) and Asplund et al. (2009).

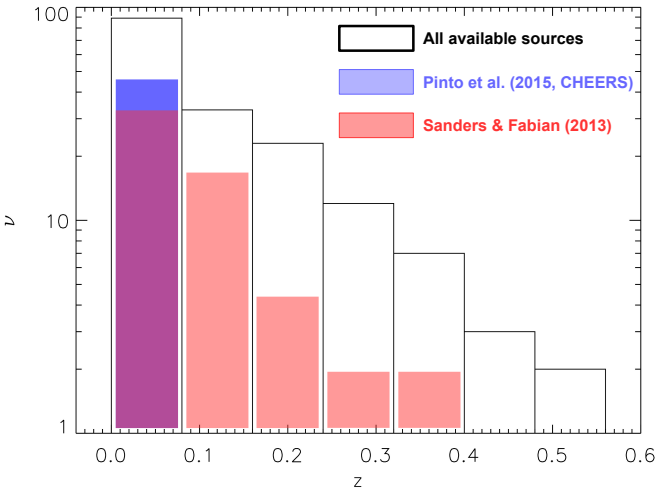

FIGURE 5 Histogram of all clusters, groups and elliptical galaxies observed with RGS at different redshift (on-axis, $t_{\rm clean} > 10$ ks, showing Fe L and / or O VIII emission lines).

X-ray energy band such X-ray calorimeters. Simionescu et al. (2019) show a remarkable example of combining the XMM-*Newton*/RGS soft X-ray and *Hitomi*/SXS hard X-ray spectra of the Perseus cluster with state-of-art atomic data, achieving an unprecedented accuracy on the relative α/Fe abundance ratios (see Fig. 4). The abundance pattern agrees with the Solar nebula and challenges any linear combinations of supernova nucleosynthesis calculations. Including neutrino physics in the yield calculations of SN cc may improve the agreement with the observed pattern of α elements in the Perseus Cluster core.

A major improvement in the measurements of both turbulence and chemical abundances will be achieved with ATHENA, the most powerful X-ray mission planned for early 2030s (see e.g. Roncarelli et al. 2018 and Cucchetti et al. 2018).

4.3 | Synergies with long wavelength facilities

The comparison of the cooling rates measured by RGS with the results obtained at lower energies is a key to unveil the evolution of the ICM. For instance, Liu et al. (2019) used the RGS observations for a sub-sample of the CHEERS catalog plus A 1835 and confirmed that the cooling rates are an order of magnitude lower than the theoretical predictions. However, they also showed that the cooling rates may still be high enough to explain the Hα luminosity and the star formation rates measured with *Hubble Space Telescope* and WISE. Pinto et al. (2018) have shown that the cooling rate of $350 \pm 130\ M_\odot\ {\rm yr}^{-1}$ below 2 keV measured with RGS in the Phoenix cluster is consistent with the star formation rate in this object and is high enough to produce the molecular gas found with ALMA in the filaments via instabilities during the buoyant rising time (see Russell, McDonald, McNamara, Fabian, & Nulsen 2017).

4.4 | Improving atomic databases

RGS has been crucial to test the accuracy of atomic databases for plasmas at $\sim$ 0.1-1 keV temperatures. de Plaa et al. (2017) and Gu et al. (2019) have shown that RGS spectra are sensitive enough to distinguish among different calculations of atomic cross sections. The ICM abundance pattern seems to agree with the Sun if state-of-art atomic databases are adopted (see Sect. 4.2 and Gu et al. 2019). Currently, there are uncertainties for 10–20% in the emissivities of the strongest emission lines. The spectral fits would appear identical in CCD spectra, but with abundances wrong by up to 20%. Finally, RGS spectra have also been able to find the first evidence for charge exchange between the cold neutral gas and the hot atmosphere in galaxy clusters (see e.g. Pinto et al. 2016 and Gu et al. 2018).

5 | CONCLUSIONS

In almost 20 years, XMM-*Newton*/RGS has delivered and continues to deliver fascinating and unique science. Here we have summarised the most crucial contribution of RGS to the astrophysics of galaxy clusters such as the accurate measurements of cooling rates, the constraints on turbulence and on cooling–heating balance, the accurate abundance measurements and the supernova yields, the tests and improvements on new atomic databases. Even now, after two decades, new scientific problems appear, triggered by the investigation of the available RGS spectra and the large databases. Whilst waiting for new missions, RGS can make significant progress by going deeper with longer exposure times and at higher redshifts closer to the peak of the star formation in the coming decade. Moreover there is a wealth of RGS data still to be studied (see Fig. 5).

ACKNOWLEDGMENTS

This work is based on observations obtained with XMM-*Newton*, an ESA science mission funded by ESA Member States and USA (NASA). We acknowledge support by European Space Agency (ESA) Research Fellowships.

REFERENCES

Ascasibar, Y., & Markevitch, M. 2006, October, *ApJ*, *650*, 102-127.
Asplund, M., Grevesse, N., Sauval, A. J., & Scott, P. 2009, Sep, *ARA&A*, *47*(1), 481-522.
Bambic, C. J., Pinto, C., Fabian, A. C., Sanders, J., & Reynolds, C. S. 2018, Jul, *MNRAS*, *478*(1), L44-L48.
Brüggen, M., Hoeft, M., & Ruszkowski, M. 2005, July, *ApJ*, *628*, 153-159.
Bulbul, G. E., Smith, R. K., Foster, A., Cottam, J., Loewenstein, M., Mushotzky, R., & Shafer, R. 2012, March, *ApJ*, *747*, 32.
Buote, D. A., Lewis, A. D., Brighenti, F., & Mathews, W. G. 2003, Sep, *ApJ*, *595*(1), 151-166.
Churazov, E., Forman, W., Jones, C., & Böhringer, H. 2000, April, *A&A*, *356*, 788-794.
Cucchetti, E., Pointecouteau, E., Peille, P. et al. 2018, Dec, *A&A*, *620*, A173.
de Plaa, J., Kaastra, J. S., Tamura, T., Pointecouteau, E., Mendez, M., & Peterson, J. R. 2004, Aug, *A&A*, *423*, 49-56.
de Plaa, J., Kaastra, J. S., Werner, N. et al. 2017, Nov, *A&A*, *607*, A98.
de Plaa, J., Werner, N., Bleeker, J. A. M., Vink, J., Kaastra, J. S., & Méndez, M. 2007, Apr, *A&A*, *465*(2), 345-355.
de Plaa, J., Zhuravleva, I., Werner, N., Kaastra, J. S., & Churazov, E. e. a. 2012, March, *A&A*, *539*, A34.
den Herder, J. W., Brinkman, A. C., Kahn, S. M. et al. 2001, Jan, *A&A*, *365*, L7-L17.
Fabian, A. C. 1994, *ARA&A*, *32*, 277-318.
Fabian, A. C., Sanders, J. S., Taylor, G. B., & Allen, S. W. 2005, June, *MNRAS*, *360*, L20-L24.
Fabian, A. C., Walker, S. A., Russell, H. R., Pinto, C., Sanders, J. S., & Reynolds, C. S. 2017, January, *MNRAS*, *464*, L1-L5.
Frank, K. A., Peterson, J. R., Andersson, K., Fabian, A. C., & Sanders, J. S. 2013, February, *ApJ*, *764*, 46.
Grange, Y. G., de Plaa, J., Kaastra, J. S., Werner, N., Verbunt, F., Paerels, F., & de Vries, C. P. 2011, Jul, *A&A*, *531*, A15.
Gu, L., Mao, J., de Plaa, J., Raassen, A. J. J., Shah, C., & Kaastra, J. S. 2018, Mar, *A&A*, *611*, A26.
Gu, L., Raassen, A. J. J., Mao, J. et al. 2019, Jul, *A&A*, *627*, A51.
Guainazzi, M., & Tashiro, M. S. 2018, July, *ArXiv e-prints*.
Hitomi Collaboration. 2016, July, *Nature*, *535*, 117-121.
Hitomi Collaboration. 2017, October, *ArXiv e-prints*.
Hudson, D. S., Mittal, R., Reiprich, T. H., Nulsen, P. E. J., Andernach, H., & Sarazin, C. L. 2010, April, *ApJ*, *513*, A37.
Kaastra, J. S., Ferrigno, C., Tamura, T., Paerels, F. B. S., Peterson, J. R., & Mittaz, J. P. D. 2001, Jan, *A&A*, *365*, L99-L103.
Kaastra, J. S., Tamura, T., Peterson, J. R. et al. 2004, Jan, *A&A*, *413*, 415-439.
Lau, E. T., Kravtsov, A. V., & Nagai, D. 2009, November, *ApJ*, *705*, 1129-1138.
Liu, H., Pinto, C., Fabian, A. C., Russell, H. R., & Sanders, J. S. 2019, May, *MNRAS*, *485*(2), 1757-1774.
Lodders, K., & Palme, H. 2009, September, *Meteoritics and Planetary Science Supplement*, *72*, 5154-+.
Matsushita, K., Fukazawa, Y., Hughes, J. P. et al. 2007, Jan, *PASJ*, *59*, 327-338.
Mernier, F., de Plaa, J., Pinto, C. et al. 2016a, Nov, *A&A*, *595*, A126.
Mernier, F., de Plaa, J., Pinto, C. et al. 2016b, Aug, *A&A*, *592*, A157.
Ogorzalek, A., Zhuravleva, I., Allen, S. W. et al. 2017, December, *MNRAS*, *472*, 1659-1676.
Peres, C. B., Fabian, A. C., Edge, A. C., Allen, S. W., Johnstone, R. M., & White, D. A. 1998, Aug, *MNRAS*, *298*(2), 416-432.
Peterson, J. R., Kahn, S. M., Paerels, F. B. S. et al. 2003, June, *A&A*, *590*, 207-224.
Peterson, J. R., Paerels, F. B. S., Kaastra, J. S. et al. 2001, January, *A&A*, *365*, L104-L109.
Pinto, C., Bambic, C. J., Sanders, J. S. et al. 2018, Nov, *MNRAS*, *480*(3), 4113-4123.
Pinto, C., Fabian, A. C., Ogorzalek, A. et al. 2016, September, *MNRAS*, *461*, 2077-2084.
Pinto, C., Fabian, A. C., Werner, N. et al. 2014, December, *A&A*, *572*, L8.
Pinto, C., Sanders, J. S., Werner, N. et al. 2015, March, *A&A*, *575*, A38.
Roncarelli, M., Gaspari, M., Ettori, S. et al. 2018, Oct, *A&A*, *618*, A39.
Russell, H. R., McDonald, M., McNamara, B. R., Fabian, A. C., & Nulsen, P. E. J. e. a. 2017, February, *ApJ*, *836*, 130.
Sanders, J. S., & Fabian, A. C. 2013, March, *MNRAS*, *429*, 2727-2738.
Sanders, J. S., Fabian, A. C., Allen, S. W., Morris, R. G., Graham, J., & Johnstone, R. M. 2008, April, *MNRAS*, *385*, 1186-1200.
Sanders, J. S., Fabian, A. C., & Smith, R. K. 2011, January, *MNRAS*, *410*, 1797-1812.
Sanders, J. S., Fabian, A. C., Smith, R. K., & Peterson, J. R. 2010, February, *MNRAS*, *402*, L11-L15.
Simionescu, A., Nakashima, S., Yamaguchi, H. et al. 2019, Feb, *MNRAS*, *483*(2), 1701-1721.
Simionescu, A., Werner, N., Böhringer, H. et al. 2009, Jan, *A&A*, *493*(2), 409-424.
Tamura, T., Bleeker, J. A. M., Kaastra, J. S. et al. 2001, Nov, *A&A*, *379*, 107-114.
Tamura, T., Kaastra, J. S., Makishima, K. et al. 2003, Feb, *A&A*, *399*, 497-504.
Urban, O., Werner, N., Allen, S. W. et al. 2017, Oct, *MNRAS*, *470*(4), 4583-4599.
Werner, N., Böhringer, H., Kaastra, J. S., de Plaa, J., Simionescu, A., Vink, J., et al. 2006, Nov, *A&A*, *459*(2), 353-360.
Werner, N., de Plaa, J., Kaastra, J. S. et al. 2006, April, *A&A*, *449*, 475-491.
Werner, N., Zhuravleva, I., Churazov, E. et al. 2009, September, *MNRAS*, *398*, 23-32.
Zhuravleva, I., Churazov, E., Schekochihin, A. A., Allen, S. W., Arévalo, P., et al. 2014, November, *Nature*, *515*, 85-87.

How cite this article: C. Pinto, J. S. Sanders, A. C. Fabian, and J. de Plaa (2019), Lessons learned from 19 years of high-resolution X-ray spectroscopy of galaxy clusters with RGS, *Astron. Nachr.*, *2019;00:1–6*.

How cite this article: C. Pinto, J. S. Sanders, A. C. Fabian, and J. de Plaa (2019), Lessons learned from 19 years of high-resolution X-ray spectroscopy of galaxy clusters with RGS, *Astron. Nachr.*, *2019;00:1–6*.